talenta PUBLISHER

Journal of Technomaterial Physics
Journal homepage: https://talenta.usu.ac.id/JoTP

Measurement and Spatial Analysis of Terrestrial Radiation in Western Peling Island

Elma Annisa Sari*, Asri Arbie, Icha Untari Meidji, Syafril Agustion Tomayahu, Siti Sarah Dayanun, and Awaludin Ismuhu

Department of Physics, Faculty of Mathematics and Natural Sciences, Gorontalo State University, Gorontalo, 96121, Indonesia

*Corresponding Author: elmaannisasarii@email.com

ARTICLE INFO

Article history:
Received 23 June 2026
Revised 19 August 2026
Accepted 28 August 2026
Available online 31 August 2026

E-ISSN: 2656-0755
P-ISSN: 2656-0747

How to cite:
E. A. Sari, A. Arbie, I. U. Meidji, S. A. Tomayahu, S. S. Dayanun, and A. Ismuhu, "Measurement and Spatial Analysis of Terrestrial Radiation in Western Peling Island," Journal of Technomaterial Physics, vol. 08, no. 02, pp. 171-178, Aug. 2026, doi: 10.32734/jotp.v8i2.26137.

ABSTRACT

Located in an archipelago characterized by carbonate rock formations, coastal environments, human settlements, and the use of locally sourced rock materials, the western part of Peling Island may exhibit a distinctive radiation pattern. This study aimed to determine the terrestrial nuclear radiation dose rate, map its spatial distribution, and evaluate whether the observed exposure levels correspond to dose limits for the general population. Field measurements were conducted using an Android-based Pocket Geiger detector with coordinate recording capability. A total of 114 observation points were established using a 1500 × 1500 m grid sampling scheme, with measurements taken at approximately ± 1 m above ground level to minimize the direct influence of ground radiation. Dose rate data (µSv/h) were analyzed descriptively to obtain maximum and average values, while spatial distribution mapping was performed using Python via Google Colab. The measured radiation dose rates were generally low, with a range of 0.00–0.24 µSv/h and an average of 0.0566 µSv/h. The estimated annual effective dose was 0.0995 mSv/year in residential areas and 0.0653 mSv/year in coastal areas, which is still below the 1 mSv/year limit recommended by ICRP and BAPETEN. These findings indicate that the study area is safe from terrestrial nuclear radiation exposure during the measurement period.

Keywords: Annual Dose, Dose Rate, Nuclear Radiation, Pocket Geiger, Spatial Mapping

ABSTRAK

Terletak di wilayah kepulauan yang dicirikan oleh formasi batuan karbonat, lingkungan pesisir, permukiman manusia, dan penggunaan material batuan yang bersumber dari lokal, bagian barat Pulau Peling mungkin menunjukkan pola radiasi yang khas. Studi ini bertujuan untuk menentukan laju dosis radiasi nuklir teresterial, memetakan distribusi spasialnya, dan mengevaluasi apakah tingkat paparan yang diamati sesuai dengan batas dosis untuk populasi umum. Pengukuran lapangan dilakukan menggunakan detektor Pocket Geiger berbasis Android dengan kemampuan pencatatan koordinat. Sebanyak 114 titik pengamatan ditetapkan menggunakan skema pengambilan sampel grid 1500 × 1500 m, dengan pengukuran diambil pada ketinggian sekitar ± 1 m di atas permukaan tanah untuk meminimalkan pengaruh langsung radiasi tanah. Data laju dosis (µSv/jam) dianalisis secara deskriptif untuk mendapatkan nilai maksimum dan rata-rata, sedangkan pemetaan distribusi spasial dilakukan menggunakan Python melalui Google Colab. Laju dosis radiasi yang diukur umumnya rendah, dengan kisaran nilai 0,00–0,24 µSv/jam dan rata-rata 0,0566 µSv/jam. Estimasi dosis efektif tahunan adalah 0,0995 mSv/tahun di daerah pemukiman dan 0,0653 mSv/tahun di daerah pesisir, yang masih berada di bawah batas 1 mSv/tahun yang direkomendasikan oleh ICRP dan BAPETEN. Temuan ini menunjukkan bahwa area studi aman dari paparan radiasi nuklir teresterial selama periode pengukuran.

Kata kunci: Dosis Tahunan, Laju Dosis, Pemetaan Spasial, *Pocket Geiger*, Radiasi Nuklir

1. Introduction

In physics, radiation refers to the process by which energy propagates through a medium or through empty space before eventually being absorbed by another body [1]. Nuclear radiation is distinguished by two fundamental properties: it is imperceptible to the human senses and it possesses sufficient energy to pass through a wide range of materials [2]. Radiation arises from both natural Its origins, such as cosmic rays and primordial radionuclides found in rock and soil, as well as man-made sources such industrial processes, mining activities, and medical equipment [3]. Based on data from the United Nations Scientific Committee on the Effects of Atomic Radiation [4], the global mean natural radiation exposure is approximately 2.4 mSv/year, though this figure varies considerably across regions owing to differences in geological composition, altitude, and anthropogenic influences. This reality underscores the need for continuous terrestrial nuclear radiation monitoring to verify that public exposure does not surpass the 1 mSv/year safety threshold established by the ICRP [5]. Despite this importance, terrestrial nuclear radiation investigations across Indonesian archipelagos and remote regions remain scarce, leaving substantial gaps in baseline radiological data for many of these locations [6].

Among the areas yet to receive dedicated environmental radiological attention is the western part of Peling Island. This region is geologically dominated by karst and carbonate rock formations, which are known to harbor naturally occurring radionuclides including ^{238}U, ^{232}Th, and ^{40}K [7]. In addition, limestone extraction may modify exposed surface materials and potentially contribute to local spatial variability, but this relationship requires direct geological and radionuclide-specific measurements to be demonstrated [8].

Field radiation measurements were carried out using an Android-based Pocket Geiger detector deployed across multiple observation sites following a systematic grid arrangement. The resulting dose rate data (in μSv/h) were subsequently processed and mapped spatially through Python scripts running on Google Colab.

Studies on the spatial distribution of terrestrial nuclear radiation across Indonesian archipelagic territories remain comparatively sparse, particularly in coastal and karst landscapes where geological variability and locally quarried construction materials create additional complexity. The limited availability of spatially referenced environmental radiation measurements in the western part of Peling Island creates a need for baseline information on terrestrial gamma radiation dose rates. This lack of spatially detailed information limits the ability to characterize the distribution of environmental radiation across the region and provides a basis for conducting systematic field measurements. Therefore, this study was conducted to provide geographically referenced baseline data on terrestrial gamma radiation dose rates in the western part of Peling Island and to describe their spatial distribution across the study area.

The primary objective of this research is to quantify and characterize terrestrial nuclear radiation dose rates across the western region of Peling Island through on-site measurements performed with an Android-based Pocket Geiger detector at numerous distributed sampling points. The collected data are then rendered as a spatially explicit radiation distribution map using Python, offering a systematic and visually interpretable depiction of the terrestrial nuclear radiation dose rate patterns across the region.

2. Research Methods

2.1. Research Equipment

An Android-based Pocket Geiger type 6 radiation detector (POKEGA), designed specifically for the direct monitoring of nuclear radiation dose rates, served as the main measuring tool used in this study. The device operates via semiconductor PIN photodiode sensor technology capable of real-time radiation detection. In practice, the POKEGA is interfaced with a smartphone through a USB connection, enabling the acquired data to be processed and stored digitally through the Pocket Geiger Type6 application. This Android-compatible system was chosen for its practicality during field surveys, ease of transport, and seamless integration with GPS functionality [9].

Beyond its role as a radiation data display interface, the Android smartphone also served as the primary device for recording geographic coordinates at each survey location. These positional records formed the essential basis for constructing the spatial radiation distribution maps. To maintain reliable data transfer and synchronization throughout the fieldwork, a wireless modem was used to sustain a stable internet connection across the research area.

The data analysis and mapping phase was conducted on a personal computer or laptop running several software tools. Microsoft Excel was applied for data tabulation and descriptive statistical processing. Google Earth was used to plot and verify the spatial positions of measurement sites, while spatial visualization and the generation of thematic radiation maps were handled through Python on the Google Colab platform. Python's scripting capabilities greatly facilitated the interpolation of numerical dose rate values and the classification of radiation intensities according to field observations.

Radiation dose rate values and the geographic coordinates of each sampling site made up the main dataset for this investigation. All data were gathered in situ using the POKEGA detector across the western region of Peling Island, which encompasses five administrative sub-districts: Bulagi, South Bulagi, North Bulagi, Buko, and South Buko. Location coordinates were acquired via the GPS sensor embedded in the mobile phone linked to the radiation detection unit.

2.2. Observation Point Determination Method

Observation sites were initially distributed using a systematic grid-based sampling approach with a cell size of 1.5 km × 1.5 km. The grid was used as the sampling framework to provide a regular and spatially distributed coverage of the study area. Within each grid cell, the final observation location was determined based on field accessibility, particularly the availability of roads or accessible pathways leading to the location. Therefore, the 114 observation points represent locations that could be safely and practically reached during field measurements, rather than all theoretical grid intersections. This accessibility constraint was necessary for field implementation but may limit the representation of areas that could not be reached, particularly locations without road access. The sampling design was consequently treated as systematic grid-based sampling with accessibility constraints [10].

Because the selection of accessible locations was constrained by the existing road network, the measured dose-rate distribution represents accessible portions of the study area and may not fully represent inaccessible terrain.

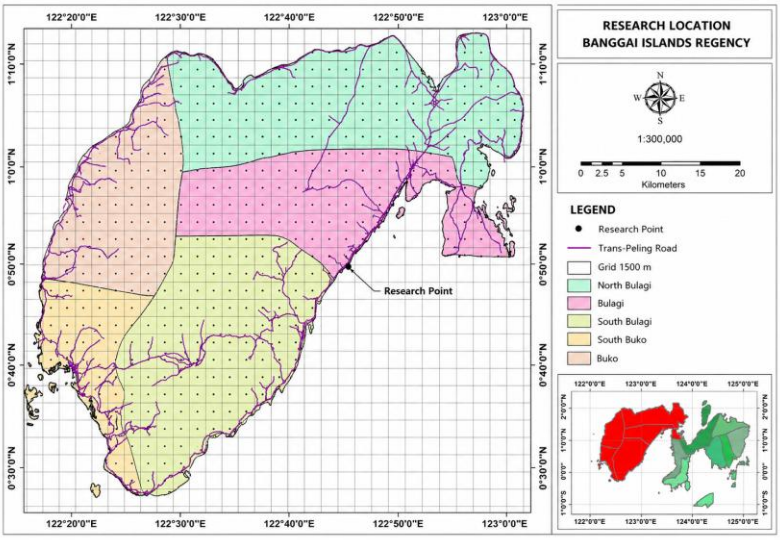

Figure 1. Research location.

Figure 1 shows the distribution of research locations in Banggai Islands Regency, particularly in the western part of Peling Island. A total of 114 measurement points were located across five administrative sub-districts: North Bulagi, Bulagi, South Bulagi, South Buko, and Buko.

2.3. Data Collection Procedure

Field data collection took place across the western region of Peling Island, spanning five sub-districts: Bulagi, North Bulagi, South Bulagi, Buko, and South Buko. Sampling locations were selected systematically using a grid-based approach, with the practical constraint that observation points were limited to areas reachable via roads or vehicle-accessible pathways. This strategy ensured a geographically balanced spread of observation points throughout the study region while allowing for efficient field mobilization. The data collected through this approach are expected to yield an accurate spatial picture of terrestrial nuclear radiation levels, supporting thorough analysis and cartographic visualization of dose rate patterns [11].

At every sampling location, the detector was held at roughly 1 m above the ground surface to suppress direct contributions from localized soil radiation and to ensure that the recorded dose rate was representative of the ambient environmental level, consistent with standards applied in prior terrestrial radiation surveys [12], [13]. Each measurement session lasted approximately 2 minutes, using the auto-recording function within the Pocket Geiger application to capture relatively stable dose rate readings. The output data encompassed radiation dose rates (μSv/h) alongside digital geographic coordinates. All field measurements were carried out under reasonably clear weather to reduce the likelihood of atmospheric interference affecting the stability of the recorded values.

Tidal fluctuations, sea breezes, and coastal erosion are some of the ongoing maritime impacts that affect coastal areas, which are transitional zones located at the border between land and water. For the purposes of this study, coastal areas are operationally defined as zones falling within ≤100 meters of the shoreline, in accordance with the coastal boundary provisions set out in Law Number 27 of 2007 [14] and Presidential Regulation Number 51 of 2016 [15]. Residential areas, by contrast, are defined as zones predominantly characterized by housing structures and everyday community activities [16], while forested areas are defined as landscapes covered predominantly by dense natural tree vegetation with little to no built development [17].

2.4. Data Processing and Analysis

All recorded measurements were compiled in tabular form and analyzed using descriptive statistics to derive the minimum, maximum, and mean at each observation point. The spatial data were then processed in Python via Google Colab, utilizing the pandas, geopandas, matplotlib, and folium libraries to generate thematic maps of terrestrial nuclear radiation distribution.

Radiation readings from residential, coastal, and forested land-cover categories were compared to identify how terrestrial nuclear radiation characteristics differ in relation to surface cover, human activity levels, and local geology. The dose rate values were then converted into annual effective doses to enable comparison against applicable radiation protection standards.

The effective annual dose was calculated using Equation (1):

$$E = \frac{D_R \times T \times OF}{1000} \tag{1}$$

where E is the annual effective dose (mSv/year), D_R is the measured terrestrial radiation dose rate, T is the total number of hours in a year (8,760 hours), OF is the occupancy factor for outdoor exposure (0.2), and the divisor 1000 converts the result from microsieverts (µSv/h) to millisieverts (mSv/year) (UNSCEAR 2000).

The calculated dose values were then benchmarked against the radiation exposure limits of 1 mSv/year for the general public as recommended by the ICRP and BAPETEN, in order to assess whether the terrestrial nuclear radiation levels in the study area can be considered radiologically safe.

3. Results and Discussion

Terrestrial nuclear radiation measurements across the Peling Island study area were conducted using an Android-based Pocket Geiger counter. The field dataset consisted of dose rate values in µSv/h together with GPS coordinates recorded at each measurement point, which were then spatially visualized through Python. Analysis of the complete dataset, covering 114 measurement points, yielded dose rates ranging from 0.00 to 0.24 µSv/h, and a mean of 0.0566 µSv/h. These findings confirm that all recorded values are low and consistent with natural background radiation levels.

As shown in Figure 2, the sampling points span residential, coastal, and forested land cover types across the western region of Peling Island. Map symbols encode the environmental radiation dose rates at each point, while the background shading reflects land surface temperature (LST) values ranging from roughly 20 to 45 °C. Forest zones are incorporated as supplementary land-cover context for the spatial visualization, though the core radiation analysis centers on residential and coastal areas. Comparable spatial radiation mapping methodologies have been described [18] and point-based dose mapping by Molnar et al. [19].

Land surface temperature (LST) data were overlaid as supplementary contextual information to help describe the broader environmental characteristics of the study area. In general, coastal and open terrain tended to show somewhat elevated surface temperatures relative to vegetated zones. However, this study did not undertake a quantitative analysis of the relationship between LST variation and changes in terrestrial nuclear radiation dose rates.

The measurement data show that average dose rates in residential areas were higher than those in coastal areas. The mean dose rate in residential settings reached 0.0568 µSv/h, while coastal areas registered a mean of 0.0373 µSv/h, confirming that residential zones carry comparatively higher ambient radiation levels. The higher dose rates observed in residential areas are likely linked to the dominant local geology, which consists of carbonate rocks and soils enriched in naturally occurring radionuclides such as uranium, thorium, and potassium. Building material selection, the density of human settlement, and specific land surface properties may further elevate dose rates in these zones. Coastal areas, in contrast, tend to record lower values, which may reflect the predominance of coastal sediment, high ambient humidity, and good air circulation, all factors that limit radionuclide accumulation at the surface.

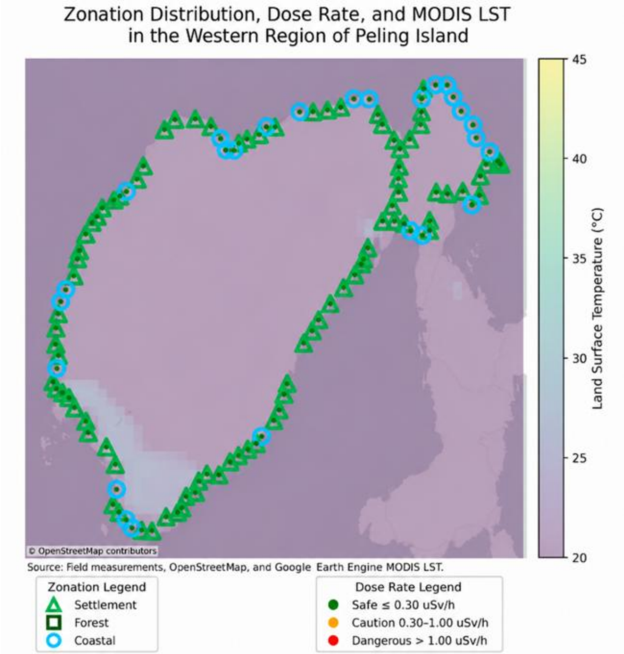

Figure 2. Spatial distribution of terrestrial nuclear radiation dose rate with land surface temperature (LST) overlay in the western region of Peling Island.

The spatial pattern in Figure 1 shows relatively minor variation between individual measurement sites. Points located in residential corridors and along roadsides consistently fell within safe exposure limits; while some residential sites showed slightly higher dose rate variability compared to coastal sites, all values remained well within safe bounds. This may be related to the use of local rocks as road or construction materials. within safe limits. This pattern may partly reflect the use of locally quarried rocks as road surfacing or construction material. Oladejo et al. noted that quarry products and surrounding soils frequently contain naturally occurring radioactive materials (NORM), especially ^{40}K, ^{232}Th, and ^{238}U, and that sites adjacent to rock material sources therefore require periodic radiological monitoring [20]. This observation is consistent with the geological setting of Peling Island, which is widely underlain by carbonate and limestone formations.

Coastal measurement sites generally produced lower dose rate readings. This pattern is likely a product of multiple interacting factors, including surface material composition, soil moisture levels, vegetation density, and the distance to exposed rock outcrops all of which influence the intensity of gamma radiation reaching the detector. Qin et al. demonstrated that natural radioactivity levels are strongly governed by lithological type, the presence of radionuclide-bearing mineral phases, and the underlying geological framework [21]. In coastal settings, Joel et al. also established that observed variability in ^{238}U, ^{232}Th, and ^{40}K activity is linked to local geological composition and anthropogenic activities at the surface [22]. Taken together, the narrow inter-point variability in dose rates suggests that terrestrial nuclear radiation throughout the study area remains governed by naturally occurring background radiation. Point-to-point differences in dose rate are tentatively attributed to site-specific geological conditions, surface material properties, and variations in land cover among the sampled locations. This finding is consistent with the karst character of the study area, where carbonate and limestone substrates are known to shape the distribution of environmental gamma radiation. From a visualization standpoint, the map provides a useful framework for interpreting the spatial interplay between sampling sites, land-use zones, and dose rate patterns. Nevertheless, the map should not be read as direct confirmation of specific radionuclide concentrations, since the measurement instrument yields only integrated dose rate values. Precise identification of ^{232}U, ^{232}Th, and ^{40}K requires gamma spectrometry, as has been demonstrated by Kr et al. [23], Bharath [18], and Oladejo et al. [20].

The mean dose rates of 0.0568 μSv/h and 0.0373 μSv/h were converted to annual effective doses using the Eq. (1). The resulting annual effective doses were 0.0995 mSv/year for residential areas (mean dose rate: 0.0568 μSv/h) and 0.0653 mSv/year for coastal areas (mean dose rate: 0.0373 μSv/h). These values were then fed into Python-based spatial visualization to generate a comprehensive map of radiation distribution across residential and coastal zones. Both figures remain below the 1 mSv/year public dose limit prescribed by the ICRP and BAPETEN (Bapeten 2013;ICRP 2007) [24]. These results are also consistent with a study by Kr et al. [23], which reported that dose rates in recreational sites around Padang remained within BAPETEN-defined safety thresholds. Nevertheless, periodic repeat measurements are advisable, as ambient dose rates can fluctuate in response to radon exhalation, rainfall, and shifting meteorological conditions [25].

3.1. The Influence of Topography and Geology on Variations In Terrestrial Nuclear Radiation Dose Rates

Fluctuations in terrestrial nuclear radiation dose rates observed across the western region of Peling Island are likely shaped by the local topographic relief and the altitudinal positions of the observation sites. Elevation data indicate that all five sub-districts within the study area Bulagi, South Bulagi, North Bulagi, Buko, and South Buko, occupy predominantly low to moderate altitudes, generally ranging between 2 and 5 meters above sea level [26]. This confirms that the study area is essentially comprised of coastal and lowland terrain, rendering any altitude-driven enhancement of cosmic radiation negligible. While it is theoretically expected that higher elevations would amplify cosmic radiation intensity due to reduced atmospheric shielding, the limited altitudinal range within the study area means this factor has minimal bearing on observed dose rate variations.

Alongside elevation, local geological conditions particularly the prevalence of carbonate and karst rock formations in the western part of Peling Island, also play a role in shaping dose rate variability. Carbonate rocks generally contain lower concentrations of natural radionuclides compared to certain igneous rock types, which helps explain why recorded dose rates fall within the low-to-normal range. Vegetation cover and the characteristics of the coastal environment further modulate radiation distribution through geochemical processes such as weathering, surface adsorption, and material leaching.

Table 1. Comparison of dose rate, AEDE, and area altitude values per district.

No	District	µSv/h	AEDE (mSv/year)	Area Height (masl)
1	Bulagi	0.0454	0.0796	3
2	Bulagi Utara	0.0461	0.0808	5
3	Bulagi Selatan	0.0526	0.0922	5
4	Buko Selatan	0.0622	0.1090	3
5	Buko	0.0641	0.1123	2

According to Table 1, the research area's terrestrial nuclear radiation radiation dose rates vary only little between districts, falling between 0.045 and 0.064 µSv/h. Buko had the greatest mean dose rate (0.0641 µSv/h and an AEDE of 0.1123 mSv/year) among the subdistricts, while Bulagi had the lowest (0.0454 µSv/h and an AEDE of 0.0796 mSv/year). Every reading is within the range of natural background radiation and is considerably below the yearly exposure limit of 1 mSv/year set by BAPETEN and the ICRP for the general public.

The differences in dose rates among sub-districts are likely driven by site-specific geological conditions, surface material properties, and local environmental characteristics. The study area, marked by carbonate rock outcrops and coastal terrain, creates conditions under which naturally occurring radionuclides such as ^{40}K, ^{232}Th, and ^{238}U can be distributed unevenly in soils and surface rocks. Additionally, the modest elevation range of 2–5 m above sea level across the area suggests that altitude-induced increases in cosmic radiation contribute minimally to the observed dose rate variability.

No measurable elevation-related increase in radiation dose rates was detected in higher-lying sub-districts such as South Bulagi and North Bulagi. Inter-sub-district variability stayed within a low range and produced no identifiable radiation anomaly zones. These patterns suggest that dose rate differences across the study area are driven more by local geological character and environmental conditions than by altitude gradients. This is consistent with findings reported by the United Nations Scientific Committee on the Effects of Atomic Radiation [27], which indicates that the distribution of natural radiation in coastal and carbonate rock environments is primarily determined by lithological composition, natural radionuclide concentrations, and surface geomorphology.

4. Conclusion

Terrestrial nuclear radiation measurements conducted across the western region of Peling Island yielded dose rates in the range of 0.00-0.24 µSv/h, with a mean value of 0.0566 µSv/h. Residential zones recorded a comparatively higher mean dose rate of 0.0568 µSv/h against 0.0373 µSv/h for coastal areas. These differences are attributed to variations in local geological conditions, surface material properties, and the degree of human activity near the measurement sites.

When dose rates were converted to annual effective doses, residential areas yielded a value of 0.0995 mSv/year while coastal areas produced 0.0653 mSv/year. Both figures remain below the 1 mSv/year radiation safety threshold for the general public as stipulated by ICRP and BAPETEN. Spatial mapping of dose rate distribution using Python indicates that the vast majority of sampling points fall within the natural background radiation category and that no significant radiological anomalies are present in the study area.

Acknowledgments

The authors would like to thank those who assisted with field data collection, measurement tools, and map processing for this study.

References

[1] Y. Sianipar, “Bahaya fisik-radiasi bagi tenaga medis dan upaya pencegahannya,” OSF Preprints, 2020, doi: 10.31219/osf.io/sberp.

[2] R. D. Saputra and V. Y. Oktavia, “Pengukuran Cacah Radiasi Nuklir dengan menggunakan Geigen Muller di Laboratorium Fisika Modern Universitas Negeri Malang,” 2020.

[3] T. M. Yoshandi, Annisa, Y. Saputra, D. R. Gavilla, and Almarinni, “Pengenalan bahaya radiasi dalam kehidupan sehari-hari: The introduction of radiation hazards in everyday’s life,” *Awal Bros J. Community Dev.*, vol. 1, no. 1, pp. 16–21, 2020, doi: 10.54973/jsabp.v1i1.21.

[4] United Nations Scientific Committee on the Effects of Atomic Radiation (UNSCEAR), *Evaluation of Medical Exposure to Ionizing Radiation*, UNSCEAR 2020/2021 Report, Vol. I, Scientific Annex A, United Nations, 2020/2021.

[5] International Commission on Radiological Protection, “The 2007 recommendations of the International Commission on Radiological Protection,” *Ann. ICRP*, vol. 37, nos. 2–4, pp. 1–332, 2007, doi: 10.1016/j.icrp.2007.10.003.

[6] Badan Pengawas Tenaga Nuklir, “Peraturan Badan Pengawas Tenaga Nuklir Nomor 4 Tahun 2024 tentang Izin Bekerja Petugas pada Fasilitas Radiasi dan/atau Kegiatan Pemanfaatan Sumber Radiasi Pengion,” Jakarta, Indonesia, 2024.

[7] N. Ngadenin, H. Syaeful, K. S. Widana, and M. Nurdin, “Potensi thorium dan uranium di Kabupaten Bangka Barat,” *EKSPLORIUM*, vol. 35, no. 2, pp. 69–84, 2014, doi: 10.55981/eksplorium.2014.8083.

[8] R. Mehra, S. Kaur, S. Chand, C. Charan, and M. Mehta, “Dosimetric assessment of primordial radionuclides in soil and groundwater of Sikar district, Rajasthan,” *J. Radioanal. Nucl. Chem.*, vol. 330, no. 3, pp. 1605–1620, 2021, doi: 10.1007/s10967-021-07998-0.

[9] A. F. Oklilas, S. D. Siswanti, and M. D. Rachman, “Akurasi Pembacaan GPS pada Android untuk Location Based Service (Studi Kasus: Informasi Lokasi SMA di Palembang),” *Jurnal Ilmu Komputer dan Agri-Informatika*, vol. 4, no. 1, pp. 1–5, 2015.

[10] Y. J. D. R. Lake, B. Pasangka, and J. L. Tanesib, “Pemetaan distribusi kandungan radioisotop di daerah perkebunan ubi kayu di Nuabosi Ende Flores,” *Jurnal Fisika: Fisika Sains dan Aplikasinya*, vol. 4, no. 2, pp. 142–152, 2019, doi: 10.35508/fisa.v4i2.975.

[11] W. A. M. Malonga, “Pemetaan distribusi penduduk Kabupaten Sumbawa dengan metode sistem grid skala ragam,” *Jurnal TAMBORA*, vol. 7, no. 2, pp. 1–7, Jul. 2023, doi: 10.36761/jt.v7i2.2985.

[12] N. Dandriyal, A. K. Sharma, and R. C. Ramola, “Measurement of terrestrial gamma exposure and radon mass exhalation rate in the soil samples of lower Kumaun Himalaya, India,” *Appl. Radiat. Isot.*, vol. 233, Art. no. 112625, 2026, doi: 10.1016/j.apradiso.2026.112625.

[13] E. Yufita, Fitriani, Fasbir, and R. Safitri, “Analisa pengaruh fungsi jarak pesawat sinar-X terhadap sebaran dosis radiasi di ruang laboratorium klinik,” *Relativitas: Jurnal Riset Inovasi Pembelajaran Fisika*, vol. 7, no. 2, pp. 94–101, 2024, doi: 10.29103/relativitas.v7i2.18234

[14] Republik Indonesia, “Undang-Undang Republik Indonesia Nomor 27 Tahun 2007 tentang Pengelolaan Wilayah Pesisir dan Pulau-Pulau Kecil,” Lembaran Negara Republik Indonesia Tahun 2007 Nomor 84, Tambahan Lembaran Negara Republik Indonesia Nomor 4739, 2007.

[15] Republik Indonesia, “Peraturan Presiden Republik Indonesia Nomor 51 Tahun 2016 tentang Batas Sempadan Pantai,” Lembaran Negara Republik Indonesia Tahun 2016 Nomor 113, 2016.

[16] M. R. Adyatma and T. S. Hadi, “Analisis penentuan lokasi perumahan oleh developer untuk masyarakat berpenghasilan rendah pada sekitar kawasan industri,” *Jurnal Kajian Ruang*, vol. 1, no. 2, pp. 198–215, 2021, doi: 10.30659/jkr.v1i2.20025.

[17] H. Hamka, A. Taiyeb, and A. Anwar, “Analisis perubahan tutupan lahan hutan di kawasan hutan lindung Desa Nupabomba menggunakan citra Landsat 8,” *ULIN: Jurnal Hutan Tropis*, vol. 9, no. 1, pp. 239–246, 2025, doi: 10.32522/ujht.v9i1.18304.

[18] K. M. Bharath, S. Bramha, S. Chandrasekaran, and M. Krishnaveni, "Geospatial assessment of natural radionuclides in urban soil of Chennai Metropolitan City," *Sci. Rep.*, vol. 15, Art. no. 40899, 2025, doi: 10.1038/s41598-025-24681-6.

[19] A. Molnar, Z. Domozi, and I. Lovas, "Drone-based gamma radiation dose distribution survey with a discrete measurement point procedure," *Sensors*, vol. 21, no. 14, Art. no. 4930, 2021, doi: 10.3390/s21144930.

[20] O. F. Oladejo, S. F. Olukotun, A. B. Rufai, and M. Mathuthu, "Assessment of radiation hazards from natural radionuclide activity in quarry sites and surrounding soils in Osun State, Southwest Nigeria," *Sci. Rep.*, vol. 15, Art. no. 19345, 2025, doi: 10.1038/s41598-025-02239-w.

[21] S. Q. Seow, P. M. Viswanathan, and D. Dodge-Wan, "Distribution of natural radioactivity in different geological formations and their environmental risk assessment in Malaysia," *Environ. Sci. Pollut. Res.*, vol. 31, no. 30, pp. 43292–43308, 2024, doi: 10.1007/s11356-024-33906-6.

[22] E. S. Joel, M. Omeje, O. C. Olawole, G. A. Adeyemi, A. Akinpelu, Z. Embong, and M. A. Saeed, "In-situ assessment of natural terrestrial-radioactivity from Uranium-238 (^{238}U), Thorium-232 (^{232}Th) and Potassium-40 (^{40}K) in coastal urban-environment and its possible health implications," *Sci. Rep.*, vol. 11, Art. no. 17555, 2021, doi: 10.1038/s41598-021-96516-z.

[23] N. Hasanah.Kr, D. Milvita, W. Wahyudi, and M. Hidayat, "Penentuan aktivitas spesifik radionuklida dan estimasi laju dosis efektif radiasi gamma di kawasan wisata Bukit Nobita Kota Padang," *Jurnal Fisika Unand*, vol. 13, no. 4, pp. 469–475, 2024, doi: 10.25077/jfu.13.4.469-475.2024.

[24] Badan Pengawas Tenaga Nuklir, "Peraturan Kepala Badan Pengawas Tenaga Nuklir Nomor 4 Tahun 2013 tentang Proteksi dan Keselamatan Radiasi dalam Pemanfaatan Tenaga Nuklir," Berita Negara Republik Indonesia Tahun 2013 Nomor 672, 2013.

[25] A. Rizzo, G. Antonacci, E. Borra, F. Cardellini, L. Ciciani, L. Sperandio, and I. Vilardi, "Environmental gamma dose rate monitoring and radon correlations: Evidence and potential applications," *Environments*, vol. 9, no. 6, Art. no. 66, 2022, doi: 10.3390/environments9060066.

[26] Badan Pusat Statistik Kabupaten Banggai Kepulauan, "Kabupaten Banggai Kepulauan dalam angka 2023," Salakan, Indonesia, 2023.

[27] United Nations Scientific Committee on the Effects of Atomic Radiation (UNSCEAR), Sources, Effects and Risks of Ionizing Radiation: UNSCEAR 2020/2021 Report, Volume II, Scientific Annex B. New York, NY, USA: United Nations, 2022.